Yang-Yang Thermodynamics on an Atom Chip

A. H. van Amerongen,[1] J. J. P. van Es,[1] P. Wicke,[1] K. V. Kheruntsyan,[2] and N. J. van Druten[1]

[1]*Van der Waals-Zeeman Institute, University of Amsterdam, Valckenierstraat 65-67, 1018 XE Amsterdam, The Netherlands*

[2]*ARC Centre of Excellence for Quantum-Atom Optics, School of Physical Sciences, University of Queensland, Brisbane, Queensland 4072, Australia*

(Received 12 September 2007; revised manuscript received 24 January 2008; published 3 March 2008)

We investigate the behavior of a weakly interacting nearly one-dimensional trapped Bose gas at finite temperature. We perform *in situ* measurements of spatial density profiles and show that they are very well described by a model based on exact solutions obtained using the Yang-Yang thermodynamic formalism, in a regime where other, approximate theoretical approaches fail. We use Bose-gas focusing [I. Shvarchuck *et al.*, Phys. Rev. Lett. **89**, 270404 (2002)] to probe the axial momentum distribution of the gas and find good agreement with the *in situ* results.

DOI: 10.1103/PhysRevLett.100.090402 PACS numbers: 05.30.Jp, 03.75.Hh, 05.70.Ce

Reducing the dimensionality in a quantum system can have dramatic consequences. For example, the one-dimensional (1D) Bose gas with a repulsive delta-function interaction exhibits a surprisingly rich variety of physical regimes that is not present in 2D or 3D [1,2]. This 1D Bose-gas model is of particular interest because exact solutions for the many-body eigenstates can be obtained using a Bethe ansatz [3]. Furthermore, the finite-temperature equilibrium can be studied using the Yang-Yang thermodynamic formalism [4–6], a method also known as the thermodynamic Bethe ansatz. This formalism is the unifying framework for the thermodynamics of a wide range of exactly solvable models. It yields solutions to a number of important interacting many-body quantum systems and as such provides critical benchmarks to condensed-matter physics and field theory [6]. The specific case of the 1D Bose gas as originally solved by Yang and Yang [4] is of particular interest because it is the simplest example of the formalism. The experimental achievement of ultracold atomic Bose gases in the 1D regime [7] has attracted renewed attention to the 1D Bose-gas problem [8] and is now providing previously unattainable opportunities to test the Yang-Yang thermodynamics.

In this Letter, we present the first direct comparison between experiments and theory based on the Yang-Yang exact solutions. The comparison is done in the weakly interacting regime and covers a wide parameter range where conventional models fail to quantitatively describe *in situ* measured spatial density profiles. Furthermore, we use Bose-gas focusing [9] to probe the equilibrium momentum distribution of the 1D gas, which is difficult to obtain through other means.

For a uniform 1D Bose-gas, the key parameter is the dimensionless interaction strength $\gamma = mg/\hbar^2 n$, where m is the mass of the particles, n is the 1D density, and g is the 1D coupling constant. At low densities or large coupling strength such that $\gamma \gg 1$, the gas is in the strongly interacting or Tonks-Girardeau regime [10]. The opposite limit $\gamma \ll 1$ corresponds to the weakly interacting gas. Here, for temperatures below the degeneracy temperature $T_d = \hbar^2 n^2/2mk_B$, one distinguishes two regimes [11]. (i) For sufficiently low temperatures, $T \ll \sqrt{\gamma} T_d$, the equilibrium state is a quasicondensate with suppressed density fluctuations. The system can be treated by the mean-field approach and by the Bogoliubov theory of excitations. The 1D character manifests itself through long-wavelength phase fluctuations resulting in a finite phase coherence length l_ϕ which greatly exceeds the mean-field correlation length l_c. (ii) The temperature interval $\sqrt{\gamma} T_d \ll T \ll T_d$ corresponds to the quantum decoherent regime [11], where both the density and the phase fluctuate. Here, the condition $l_c \ll l_\phi$ required for the existence of a quasicondensate is no longer satisfied, and the system can be treated as a degenerate ideal gas combined with perturbation theory in g. At temperatures near the crossover to the quasicondensate, $T \sim \sqrt{\gamma} T_d$, neither of the approximate approaches work, and one has to rely on the numerical solution to the exact Yang-Yang equations, as we show in the present work.

Experiments on 1D gases are usually carried out in harmonic traps with strong transverse confinement and weak confinement along the axis, $\omega_\perp \gg \omega_\parallel$. A trapped gas is in the 1D regime if both temperature and chemical potential are small with respect to the radial excitation energy, $k_B T$, $\mu \ll \hbar\omega_\perp$. It was recognized early on that the physics of the degenerate part of the trapped cloud is already effectively 1D if the weaker condition $\mu < \hbar\omega_\perp$ is satisfied [7]. For a gas in the 1D regime, the effective 1D coupling can be expressed through the 3D scattering length a as $g \simeq 2\hbar\omega_\perp a$ if $a \ll (\hbar/m\omega_\perp)^{1/2}$ [12].

Various physical regimes of a harmonically trapped 1D gas have been discussed in Refs. [1,13–15]. The above classification of the regimes for the uniform gas can be applied locally to the trapped gas if the conditions for the local density approximation (LDA) are met [1,14,15]. The

trapped cloud is then characterized by a global temperature and a spatially varying density, $n \rightarrow n(x)$. Thus, a trapped 1D gas which is in the quasicondensate regime in its center [$T \ll \sqrt{\gamma(0)} T_d(0)$] will cross over towards the wings—through the quantum-decoherent regime—to the nondegenerate regime [$T_d(x) \ll T$] as the local density $n(x)$ decreases.

We experimentally investigate the behavior of a weakly interacting trapped Bose gas [$\gamma(0) \simeq 10^{-2}$] in the regime where $\mu < \hbar\omega_\perp$ and $k_B T \simeq \hbar\omega_\perp$. Similar measurements to our *in situ* data were previously performed at higher temperatures and higher linear densities [16,17]; the observed density profiles were found to be in disagreement with approximate theories. Our approach here is different in that we present a full description of the density profiles through a consistent model based on the solutions to the exact Yang-Yang equations [4,11] and that we compare real-space and momentum-space distributions for the same experimental parameters.

For (nearly) 1D clouds, it is difficult to probe the axial momentum distribution. The conventional time-of-flight method does not work, mainly because the cloud hardly expands axially beyond its initial length. The analysis is further complicated by strong density fluctuations that develop in time of flight from the initial phase fluctuations [18]. The axial momentum distribution of phase-fluctuating 3D condensates has been measured using Bragg spectroscopy [19], but this technique is extremely sensitive to vibrations and requires averaging over many realizations.

We gain experimental access to the axial momentum distribution using Bose-gas focusing. This is a technique introduced for nonequilibrium 3D condensates [9]; here, we extend it to study the equilibrium properties of (nearly) 1D clouds. A detailed analysis of focusing in this regime will be presented elsewhere. In brief, we apply a short, strong axial harmonic potential yielding a kick to the atoms proportional to their distance from the trap center (analogous to the action of a lens in optics), followed by free propagation. As a result, the atoms come to a focus, at which time the axial density distribution reflects the axial momentum distribution before focusing. Initial phase fluctuations result in a finite width of the cloud [9]. Since the focusing brings all atoms together axially, the signal level is high, even for a single realization. As we will show, averaging over a few shots is sufficient to obtain high signal-to-noise ratio.

The core of our setup is a magnetic microtrap consisting of three layers of current carrying wires. The surface layer is formed by a silicon substrate coated with a 1.8 μm-thick vapor-deposited patterned gold layer. This atom chip faces in the direction of gravity ($+z$). On the chip, we use a Z-shaped wire, with a 3 mm long and 125 μm wide central section along x. The remaining two layers are behind the silicon substrate, and each contains three parallel copper wires (diameter 300 μm), in the x and y-direction, centered at $z = -0.5$ mm and -0.8 mm from the chip surface, respectively. The wires in the y direction are used to vary the confinement along x.

We trap 2×10^7 ^{87}Rb atoms in the $F = 2$, $m_F = 2$ state in a tight magnetic trap near the chip surface, and perform forced evaporative cooling by applying a radio frequency (rf) field. The frequency ω_{rf} is ramped down from 27 to 1.7 MHz relatively quickly (in 180 ms) to purposely reduce the atom number, in order to penetrate deeper into the 1D regime. Before reaching degeneracy, we relax the axial confinement to a final trap with $\omega_\perp/2\pi = 3280$ Hz, $\omega_\parallel/2\pi = 8.5$ Hz, and a bottom corresponding to $\omega_{\mathrm{rf}}/2\pi = 1.518(2)$ MHz. The current in the Z-wire is set at 2.25 A, and the distance of the cloud to the chip surface is 90 μm. In this trap, we perform a slower ramp (450 ms) to the final rf frequency. An additional 300 ms of plain evaporation allows the damping of residual quadrupole collective oscillations in the cloud to the point where these oscillations are no longer visible. We probe the gas using standard absorption imaging, with a measured optical resolution limit of 4 μm. The CCD camera square pixel size is 2.15 μm in the object plane. Our axial trapping potential was characterized using both the measurement of *in situ* density profiles at high T and the dipole mode oscillation frequency in the trap center. The curvature in the center corresponds to a frequency of 8.5 Hz and gradually decreases to $\sim$6 Hz in the wings of the cloud [20].

In Figs. 1(a)–1(d), we show the linear density of atomic clouds in the magnetic trap for different final rf frequencies. These data were obtained by *in situ* absorption imaging and integrating the atom number along z. The absolute atom number was calibrated using time-of-flight data. Each curve is an average of $\sim$18 images taken under identical circumstances. Since all of our data was taken for $\mu < \hbar\omega_\perp$ [21], we expect that the interactions will significantly affect only the distribution in the radial *ground* state, while the population in the radially *excited* states can to a good approximation be described by the ideal-gas distribution. This leads to the following model that was used to analyze the *in situ* data.

We start from the solution to the Yang-Yang integral equations for a finite-temperature uniform 1D Bose gas at thermal equilibrium [4]. This yields numerical results for both the equation of state $n_{\mathrm{YY}}(\mu, T)$ and the local pair correlation [11]. The LDA is then used to account for the axial potential via a varying chemical potential $\mu(x) = \mu - V(x)$. This approach is expected to be valid as long as the axial potential is smooth on the scale of the relevant correlation lengths [14,15]. Since our temperature is on the order of the radial level splitting, $\hbar\omega_\perp/k_B = 158$ nK, the fraction of the gas which occupies radially excited states can not be neglected. We account for this fraction by summing over radially excited states (radial quantum number $j \geq 1$, degeneracy $j + 1$) and treating each radial state as an independent ideal 1D Bose gas in thermal equilib-

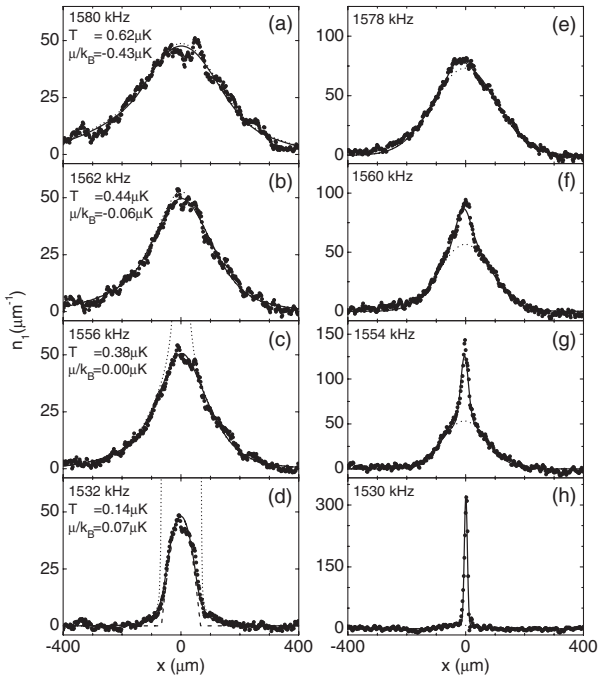

FIG. 1. Linear atomic density from absorption images obtained *in situ* (a)–(d) and *in focus* (e)–(h) by lowering (from top to bottom as indicated) the final rf evaporation frequency. *In situ*: solid lines are fits using Yang-Yang thermodynamic equations (see text). The values of μ and T resulting from the fits are shown in the figure. Dotted line: ideal Bose-gas profile showing divergence for $\mu(x) = 0$. Dashed line in (d): quasicondensate profile with the same peak density as the experimental data. *In focus*: solid lines are the sum of two independent Gaussian fits—one to the wings (dotted lines) and one to the central part of the density profile.

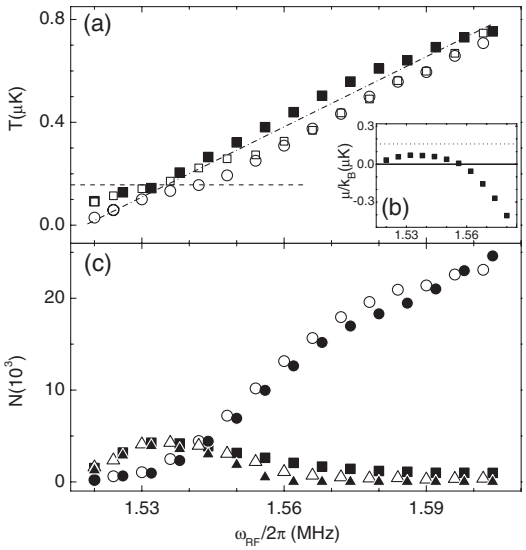

FIG. 2. Characterization of the atomic clouds as a function of the final rf frequency, as determined from fits of the Yang-Yang model to the *in situ* data and Gaussian fits to the *in focus* data. (a) Temperature from the *in situ* data (■) and from the radial (□) and axial (○) size of the broad Gaussian fit to the *in focus* data. The dash-dotted line is to guide the eye and indicates a ratio of 11 of the trap depth and the cloud temperature; dashed line corresponds to $\hbar\omega_\perp/k_B$. (b) Chemical potential from the Yang-Yang fit; dashed line indicates $\hbar\omega_\perp/k_B$. (c) Atom number from the *in focus* data: wide distribution (○) and central peak (△); from the Yang-Yang model fit to the *in situ* data: atoms in the radial ground state (■), in radially excited states (•), and atoms in the radial ground state experiencing $\mu(x) > 0$ (▲).

rium with the gas in the radial ground state, $\mu_j(x) = \mu(x) - j\hbar\omega_\perp$ [22]. Within this model, the linear density is given by

$$n_1(x, \mu, T) = n_{\mathrm{YY}}[\mu(x), T] + \sum_{j=1}^{\infty}(j+1)n_e[\mu_j(x), T].$$

For the radially excited states, we use the result of the LDA for the 1D ideal gas, $n_e(\mu_j, T) = g_{1/2}[\exp(\mu_j/k_BT)]/\Lambda_T$ where $g_{1/2}$ is a Bose function and $\Lambda_T = (2\pi\hbar^2/mk_BT)^{1/2}$ is the thermal de Broglie wavelength [1,15]. Note that as long as $\mu < \hbar\omega_\perp$, we have $\mu_j < 0$ which is necessary to avoid divergence of $g_{1/2}$. In this model, the radially excited states act as a bath for particle and energy exchange with the radial ground state. The resulting fits are shown as solid lines in Figs. 1(a)–1(d) and describe our data very well. The fitted values of T and μ are displayed in Fig. 2.

We now turn to the *in focus* measurements which give access to the axial momentum distribution of the gas. The focusing pulse is created by ramping up the axial trapping frequency from 8.5 to 20 Hz in 0.8 ms, maintaining this for 3.8 ms, and ramping back to 8.5 Hz in 0.8 ms, followed by a sudden switch-off of the magnetic trap. During the focusing pulse, the cloud length reduces by less than 20%. After switching off the magnetic trap, the cloud expands in the radial direction on a time scale of $1/\omega_\perp$ so that the interactions vanish rapidly compared to the relevant axial time scale, and the subsequent axial contraction can be treated as free propagation. After 13 ms of free propagation, the cloud comes to a focus.

In Figs. 1(e)–1(h), we show the axial density distribution obtained in the focus, averaged over typically 10 shots, for final rf frequencies similar to the *in situ* data in Figs. 1(a)–1(d). Here, in contrast to the *in situ* results, one can clearly distinguish a narrow peak from a broad pedestal for rf values below 1.56 MHz [Figs. 1(g) and 1(h)]. The Yang-Yang solution does not yield the momentum distribution, and thus it can not be used to fit to the *in focus* data. Instead, to quantify the observation of the bimodal structure, we first fit a 2D Gaussian to the wings of the atomic density distribution. In a second step, we fit a narrow Gaussian to the residual peak in the center. The fitted curves are shown after integration in the z direction in Figs. 1(e)–1(h), and describe the observed *in focus* distributions well. Figure 2(c) shows the resulting atom numbers in the wide and narrow part of the momentum distribution; we also plot the atom numbers from the Yang-Yang model in the radial ground state, in the radially excited states, and atoms in the radial ground state experiencing $\mu(x) > 0$. Comparing the *in situ* and the *in focus* data, we conclude

that (i) the momentum distribution becomes bimodal around the point where the global chemical potential μ crosses zero and becomes positive, and (ii) the narrow part of the momentum distribution is dominated by the atoms in the radial ground state (described by n_{YY}), while the wide part is dominated by atoms in the radially excited states. The shape of the narrow peak thus constitutes a measurement of the momentum distribution of the Yang-Yang gas, for which currently no theoretical comparison is available.

A further comparison between the *in focus* and *in situ* results can be made as follows. Estimates for the temperature can be obtained from the Gaussian fit to the wide part of the *in focus* data, by assuming that the tails (where degeneracy is negligible) are well described by Boltzmann statistics. The resulting temperatures are shown in Fig. 2(a). The agreement with the temperature extracted from the *in situ* data is reasonable. We attribute the remaining discrepancy to the approximations implicit in the above interpretation of the Gaussian fit results, which neglects the discrete radial level structure and the contribution of the radial ground state to the wide part of the axial momentum distribution.

The failure of the ideal-gas and quasicondensate descriptions is illustrated in Figs. 1(c) and 1(d). The key point here is the following. The Yang-Yang thermodynamic equations yield a smooth equation of state $n_{YY}(\mu, T)$, including the region around $\mu(x) = 0$. This deviates dramatically from both the ideal-gas description (diverging density as $\mu \to 0$ from below) and the quasicondensate description (vanishing density as $\mu \to 0$ from above). The region in $\mu(x)$ [and consequently in $n_{YY}(x)$] where this discrepancy is significant [15] is particularly large for our parameters, and the Yang-Yang thermodynamic solutions are essential for a proper description of the data.

In conclusion, we have found excellent agreement between *in situ* measurements of the spatial linear density of a nearly 1D trapped Bose gas and a model based on the exact Yang-Yang solutions. We have measured the corresponding momentum distribution and expect this to stimulate further theoretical work. More generally, our results establish a new and strong link between experiments on low-dimensional quantum gases and exact theory for interacting quantum many-body systems at finite temperatures, both fields of significant current interest. Additionally, our findings should be relevant to related experimental systems, such as guided-wave atom lasers [23] and atom-chip based interferometers [24].

We thank J. T. M. Walraven, G. V. Shlyapnikov, and J.-S. Caux for fruitful discussions. The atom chip was produced at the Amsterdam nanoCenter. This work was funded by FOM, NWO, and by the EU (No. MRTN-CT-2003-505032). K. K. acknowledges support by the Australian Research Council, the Queensland State Government, and the Institut Henri Poincaré—Centre Emile Borel.

[1] D. S. Petrov, D. M. Gangardt, and G. V. Shlyapnikov, J. Phys. IV (France) **116**, 5 (2004), and references therein.
[2] Y. Castin, J. Phys. IV (France) **116**, 89 (2004).
[3] E. H. Lieb and W. Liniger, Phys. Rev. **130**, 1605 (1963).
[4] Yang and Yang, J. Math. Phys. (N.Y.) **10**, 1115 (1969).
[5] V. E. Korepin, N. M. Bogoliubov, and A. G. Izergin, *Quantum Inverse Scattering Method and Correlation Functions* (Cambridge University Press, Cambridge, England, 1993).
[6] M. Takahashi, *Thermodynamics of One-Dimensional Solvable Models* (Cambridge University Press, Cambridge, England, 1999).
[7] A. Görlitz *et al.*, Phys. Rev. Lett. **87**, 130402 (2001); F. Schreck *et al.*, *ibid.* **87**, 080403 (2001); M. Greiner *et al.*, *ibid.* **87**, 160405 (2001); H. Moritz *et al.*, *ibid.* **91**, 250402, (2003); B. Laburthe Tolra *et al.*, *ibid.* **92**, 190401 (2004).
[8] J. O. Andersen *et al.*, Phys. Rev. Lett. **88**, 070407 (2002); G. E. Astrakharchik *et al.*, *ibid.* **92**, 030402 (2004); C. Menotti and S. Stringari, Phys. Rev. A **66**, 043610 (2002); M. A. Cazalilla, *ibid.* **67**, 053606 (2003); J.-S. Caux and P. Calabrese, *ibid.* **74**, 031605 (2006).
[9] I. Shvarchuck *et al.*, Phys. Rev. Lett. **89**, 270404 (2002).
[10] M. D. Girardeau, J. Math. Phys. (N.Y.) **1**, 516 (1960); T. Kinoshita, T. Wenger, and D. S. Weiss, Science **305**, 1125 (2004); B. Paredes *et al.*, Nature (London) **429**, 277 (2004).
[11] K. V. Kheruntsyan *et al.*, Phys. Rev. Lett. **91**, 040403 (2003).
[12] M. Olshanii, Phys. Rev. Lett. **81**, 938 (1998).
[13] D. S. Petrov, G. V. Shlyapnikov, and J. T. M. Walraven, Phys. Rev. Lett. **85**, 3745 (2000).
[14] K. V. Kheruntsyan *et al.*, Phys. Rev. A **71**, 053615 (2005).
[15] I. Bouchoule, K. V. Kheruntsyan, and G. V. Shlyapnikov, Phys. Rev. A **75**, 031606(R) (2007).
[16] J. Estève *et al.*, Phys. Rev. Lett. **96**, 130403 (2006).
[17] J.-B. Trebbia *et al.*, Phys. Rev. Lett. **97**, 250403 (2006).
[18] These fluctuations have been studied in detail for elongated 3D condensates with $\mu > \hbar\omega_\perp$; S. Dettmer *et al.*, Phys. Rev. Lett. **87**, 160406 (2001), and [19].
[19] S. Richard *et al.*, Phys. Rev. Lett. **91**, 010405 (2003).
[20] We attribute this anharmonicity to small, long-wavelength deviations from straight current flow in the trapping wire [D. W. Wang *et al.*, Phys. Rev. Lett. **92**, 076802 (2004); J. Estève *et al.*, Phys. Rev. A **70**, 043629 (2004)]. Disturbances at high spatial frequencies are negligible because of the large trapping distance (90 μm) from the chip. We used the following potential in our model: (i) $V(x) = m\omega^2 x^2/2$ with $\omega/2\pi = 8.5$ Hz for $|x| < 130$ μm, (ii) $V(x) = m\omega_w^2(x + x_w)^2/2 + V_w$ with $\omega_w/2\pi = 5.4$ Hz, $x_w = 26$ μm, $V_w/k_B = 395$ nK for $|x + x_w| > 325$ μm, and (iii) a third-order-polynomial interpolation between these two ranges.
[21] The condition $\mu < \hbar\omega_\perp$ is satisfied if $n_1 < 3/4a \simeq 150$ μm^{-1}, F. Gerbier, Europhys. Lett. **66**, 771 (2004).
[22] This is similar to the approach used by M. Naraschewski and D. M. Stamper-Kurn, Phys. Rev. A **58**, 2423 (1998).
[23] W. Guerin *et al.*, Phys. Rev. Lett. **97**, 200402 (2006).
[24] S. Hofferberth *et al.*, Nature (London) **449**, 324 (2007).